

Observations of Atmospheric Dynamics using Radar Techniques*

B. H. Briggs

Department of Physics and Mathematical Physics, University of Adelaide,
G.P.O. Box 498, Adelaide, S.A. 5001, Australia.

Abstract

A surprisingly large amount of information about atmospheric dynamics can be obtained by studying the fluctuations of the amplitude and phase of radar echoes back-scattered from density irregularities. The method has been extensively used by the Atmospheric Physics Group at the University of Adelaide, and elsewhere. In the present paper these techniques are traced back to their origin in the pioneering work of J. L. Pawsey in the 1930s, and followed through to the present day. The reasons which led to the construction of the large antenna array near Adelaide (the 'Buckland Park array') are explained, and the observations which can be made with it are described. These include radar measurements of winds, turbulence and momentum flux in the height range 60 to 95 km. Plans for instrumental improvements and for future work are outlined. The paper is not intended to be a general review of the field, but rather a history of a technique and its development in the research groups with which the author has been associated.

1. Introduction: The Work of J. L. Pawsey

This paper will adopt a historical approach. I propose to trace the history of a group of radar techniques which have been used extensively by the Atmospheric Physics Group at the University of Adelaide. The group has used many other techniques over the years, not included in the present paper; for example, radar observations of meteor trails, and lidar and acoustic sounding of the atmosphere. However, the techniques to be described have always formed a continuing and central component of the work, and the largest instrument of the group, the 'Buckland Park array', was built to exploit these techniques. They involve study of the 'fading' (i.e. temporal fluctuations of amplitude and phase) of radar echoes returned from atmospheric inhomogeneities. The aim is to discover what these fluctuations can tell us about atmospheric dynamics, and to derive the maximum possible amount of information from them.

The fading of radio signals has been observed ever since radio waves were first used for communication, but from the point of view of the present paper the seminal work was undoubtedly that of J. L. Pawsey carried out in the 1930s. Pawsey graduated from Melbourne University and went to Cambridge in 1931 to work in J. A. Ratcliffe's radio group at the Cavendish Laboratory. (It is of interest that H. S. W. Massey did the same just two years earlier; he went to work under Rutherford.) Ratcliffe gave Pawsey the task of finding out more

* Harrie Massey Prize Lecture presented at the Tenth AIP Congress, University of Melbourne, 13 February 1992.

about the causes of the fading of echoes reflected from the ionosphere. The fluctuations appeared to be random, and had fading times of the order of seconds. Pawsey decided to find out over what horizontal distances the fluctuations were correlated, and to do this he set up two radio receivers whose separation could be varied. It was necessary to record the echo strengths on the same chart, and in his paper (Pawsey 1935) he describes how this was done:

'The intensity variations of the chosen echo were recorded by a semi-automatic device which worked in the following manner. Potentiometers were arranged at each receiver, the outputs from which, carried by lines to a common point, actuated two Einthoven galvanometers which recorded the potentiometer settings on the same moving film. To each potentiometer was attached a pointer which moved over the region on the face of the oscillograph in which the echo under study was situated. An observer at each receiver continually adjusted his pointer to coincide with the tip of the echo pattern, and so recorded the intensity changes.'

The key observation was that on one occasion, for a receiver spacing of 140 m, the intensity changes were similar but showed a consistent time displacement of about 1 s. Pawsey interpreted this as evidence for a wind at the level of reflection of the radio wave. He used diffraction theory to show that if the reflecting stratum behaves as a random diffracting screen, then moving the screen a certain distance will cause the diffraction pattern formed on the ground to move twice as far. Therefore, he halved the velocity of 140 ms^{-1} to obtain a wind speed of 70 ms^{-1} at the reflection level. This factor of 2 arises because the upgoing radio wave is not a plane wave but comes from a point source; it later became known as the 'point-source effect'. (For future reference, it is useful to note that a geometrically equivalent statement of the point-source effect is the following: if the source moves a distance $-X$, the screen being stationary, then the diffraction pattern moves $+X$. In this form the result can be experimentally tested; see Section 3.)

In another application of diffraction theory, Pawsey showed in the 1935 paper that observations of the scale of the diffraction pattern formed over the ground could be used to deduce the degree of angular spreading of the downcoming radio waves. For a smooth reflector, waves would be returned only from the zenith, but for the actual ionosphere Pawsey showed that back-scattering occurs for angles up to $\pm 20^\circ$ off-zenith.

At this point the investigations appear to have ceased, probably because of the looming Second World War. There were more urgent radar matters to be attended to than winds in the upper atmosphere.

2. Work at Cambridge, 1946–1962

Ratcliffe returned to Cambridge from wartime radar work in 1946 and started to re-establish his research group at the Cavendish. I joined his group as a research student shortly afterwards. Ratcliffe wished to follow up Pawsey's method as a means of measuring winds in the upper atmosphere, few other methods being available at that time. Several research students were involved in this line of work (S. A. Bowhill, B. H. Briggs, S. N. Mitra, G. J. Phillips, D. H. Shinn and later M. Spencer). We soon realised that there was a problem in applying the

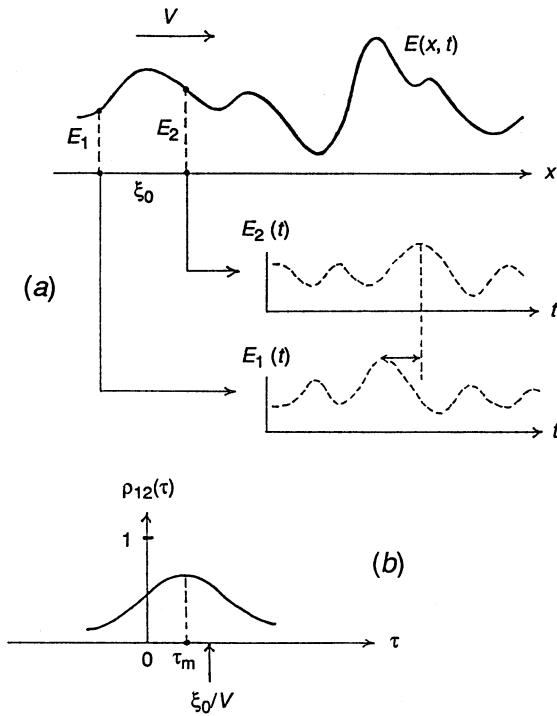


Fig. 1. (a) A changing pattern $E(x, t)$ moves with velocity V past two antennas to produce records $E_1(t)$ and $E_2(t)$. (b) The cross-correlation function $\rho_{12}(\tau)$ between $E_1(t)$ and $E_2(t)$ has a maximum value at a lag τ_m , smaller than the 'correct' value ξ_0/V .

method in its simple form because, unless the atmospheric motion is completely non-turbulent, the diffraction pattern on the ground will change in form as it moves. (Pawsey himself had suggested that turbulence as well as winds might well be an important cause of fading.) In this case it is not difficult to show that the velocity obtained by dividing the receiver separation by the time displacement of the fading curves will give a velocity which is too large.

In order to see this consider the situation shown in Fig. 1a. Two antennas, separated by a distance ξ_0 , are used to record the signal strengths $E_1(t)$ and $E_2(t)$ due to the passage of the pattern $E(x, t)$. This pattern is assumed to move with a velocity V along the x -axis, but also changes as it moves. [We consider a one-dimensional case for simplicity; the real pattern is, of course, two-dimensional. Also, we assume that just the amplitude of $E(x, t)$ is recorded, so that $E_1(t)$ and $E_2(t)$ are real. In early work the phase was not used, but in most recent work both amplitude and phase are used and combined to form complex time series.]

The time displacement between $E_1(t)$ and $E_2(t)$ is best found by plotting the correlation coefficient between the two time series as a function of the relative

shift τ . This function $\rho_{12}(\tau)$ is called the cross-correlation function, and its form is shown in Fig. 1*b*. Suppose it has a maximum for a time shift τ_m . This time shift tells us the time difference which makes the two time series resemble each other most closely. The maximum correlation will be less than unity, because the pattern $E(x, t)$ is changing as it moves, and so the detailed shapes of the fluctuations $E_1(t)$ and $E_2(t)$ will be different. More important, the time shift τ_m will be *less* than the 'correct' value ξ_0/V . This is because, by introducing a smaller time shift than the 'correct' one, we reduce the amount of random change, and therefore obtain a higher correlation. Indeed, if $V = 0$, so that the only temporal changes are the random ones, the cross-correlation function will have its maximum at $\tau_m = 0$. A pattern of this type can be visualised as being like the surface of boiling porridge.

Although we know that τ_m is going to be less than the 'correct' value, we can still define an 'apparent' velocity V' as

$$V' = \xi_0/\tau_m, \quad (1)$$

but we expect V' to be greater than V , unless the atmospheric motion is completely non-turbulent.

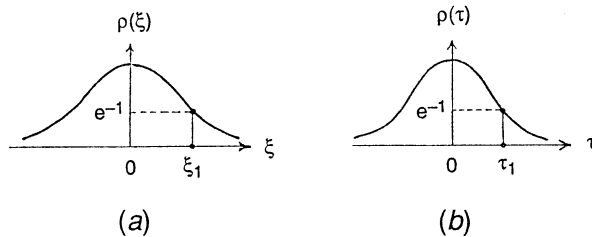


Fig. 2. (a) The form of the spatial correlation function for a random pattern with a characteristic scale ξ_1 . (b) The form of the temporal correlation function for a pattern with a characteristic time scale (or lifetime) τ_1 .

It thus became clear that, in order to obtain the correct wind velocity, a model was needed by means of which a correction could be applied to allow for the effects of the random changes. Consider first a pattern which changes randomly, but does not move systematically (like the boiling porridge mentioned above). Such a pattern will have a characteristic spatial scale, and a characteristic time scale. For a Gaussian model, we can write the 'spatio-temporal' correlation function as

$$\rho(\xi, \tau) = \exp \left\{ - \left(\frac{\xi^2}{\xi_1^2} + \frac{\tau^2}{\tau_1^2} \right) \right\}, \quad (2)$$

where ξ is a spatial increment, and τ a time increment. Thus, if at one instant ($\tau = 0$) we were to plot the correlation coefficient as a function of antenna separation ξ , we would obtain a spatial correlation function of the form shown in Fig. 2*a*. The separation ξ_1 at which the correlation falls to e^{-1} is a good

definition of the pattern's characteristic scale. Conversely, if at one point ($\xi = 0$) we were to plot the correlation as a function of temporal shift τ , we would obtain a curve like that in Fig. 2*b*. This is usually called the autocorrelation function, $\rho_{11}(\tau)$. The time shift τ_1 for which the correlation falls to e^{-1} is a good measure of the characteristic time scale (or lifetime) of the random temporal fluctuations.

Now consider the same pattern moving over the ground with velocity V . An observer moving with the pattern would still describe it by equation (2). However, an observer fixed with respect to the ground would have to make the coordinate transformation

$$x' = x + Vt, \quad t' = t,$$

and so the spatial and temporal increments ξ', τ' for the fixed observer would be related to those for the moving observer by

$$\xi' = \xi + V\tau, \quad \tau' = \tau. \quad (3)$$

Making these substitutions in (2) we obtain

$$\rho(\xi', \tau') = \exp \left\{ - \left(\frac{(\xi' - V\tau')^2}{\xi_1^2} + \frac{\tau'^2}{\tau_1^2} \right) \right\}. \quad (4)$$

This is the basic equation we need to describe a pattern which moves with velocity V and also changes as it moves. For future use, we now drop the primes in (4).

Consider now the application of this model to an experiment of the type carried out by Pawsey, and suppose the antenna separation is ξ_0 . The predicted cross-correlation function $\rho_{12}(\tau)$ is

$$\rho_{12}(\tau) = \rho(\xi_0, \tau) = \exp \left\{ - \left(\frac{(\xi_0 - V\tau)^2}{\xi_1^2} + \frac{\tau^2}{\tau_1^2} \right) \right\}. \quad (5)$$

By differentiating with respect to τ , this can be shown to have a maximum value for

$$\tau = \tau_m = \frac{\xi_0 V}{V^2 + \xi_1^2/\tau_1^2} \quad (6)$$

(see Fig. 1*b*). The apparent velocity V' is therefore

$$V' = \frac{\xi_0}{\tau_m} = \frac{V^2 + \xi_1^2/\tau_1^2}{V}. \quad (7)$$

This is clearly greater than V , as expected, unless the term ξ_1^2/τ_1^2 is zero. The only way this term can be zero is if $\tau_1 \rightarrow \infty$, i.e. the random changes are characterised by an infinite lifetime, which just means that the pattern is not changing as it moves.

We cannot find all the unknowns in the model just by fitting (5) to the observed cross-correlation function. However, we can also observe the autocorrelation function, by using the time series obtained at one point, and correlating it with itself for variable time displacements (Fig. 2*b*). According to the model, this function is given by

$$\rho_{11}(\tau) = \rho(0, \tau) = \exp \left\{ - \left(\frac{V^2}{\xi_1^2} + \frac{1}{\tau_1^2} \right) \tau^2 \right\}. \quad (8)$$

By fitting the *observed* cross- and autocorrelation functions to (5) and (8), it is a straightforward matter to determine the three unknowns of the theory, namely ξ_1 , τ_1 and V . Note that V is the true velocity. All three quantities are of practical interest.

The pattern scale ξ_1 is related, as Pawsey showed, to the extent of the angular spreading of the downcoming radio waves. In fact, the angular power spectrum as a function of s/λ (where s is the sine of the off-zenith angle θ and λ is the radar wavelength) can be shown to be the Fourier transform of the spatial correlation function $\rho(\xi)$ (Ratcliffe 1956). For the present model with $\rho(\xi) = \exp(-\xi^2/\xi_1^2)$, the angular power spectrum $W(s)$ is therefore given by

$$W(s) \propto \exp(-s^2/s_0^2), \quad (9)$$

where

$$s_0 = \lambda/\pi\xi_1. \quad (10)$$

The pattern lifetime τ_1 is related, as will be shown in Section 6, to the turbulent velocities of the atmospheric scatterers, and hence to the turbulent energy dissipation rate. The true pattern velocity V gives, of course, the horizontal wind velocity $\frac{1}{2}V$.

This model needs to be extended to the two-dimensional case and to a triangle of three receiving antennas in order to be applicable in practice. This extension is straightforward and will not be given here. It does introduce one new feature; the pattern need not be isotropic in the sense that its 'scale' is the same in all directions. It may be systematically elongated in a particular direction, which is related to a corresponding elongation of the scatterers. This possibility is allowed for in the full theory, and parameters describing the degree and the direction of the elongation are derived.

The correlation technique described above is equivalent to that in the original papers (Briggs *et al.* 1950; Phillips and Spencer 1955), but presented rather differently in a way which I hope is easier to follow. A similar treatment for the two-dimensional case can be found in Briggs (1984). The general theory does not assume that the correlation functions are Gaussian, but allows them to be of a general form. The Gaussian functions were introduced here mainly to simplify the explanation; however, we will see in Section 5 that there may be some theoretical justification for assuming this form.

The theory was never extensively employed at Cambridge because at that time digitisation of records had to be done by hand and was very tedious; electronic computers also were in their infancy. Some use was made of EDSAC, the early computer at Cambridge, which used valves. The results showed that

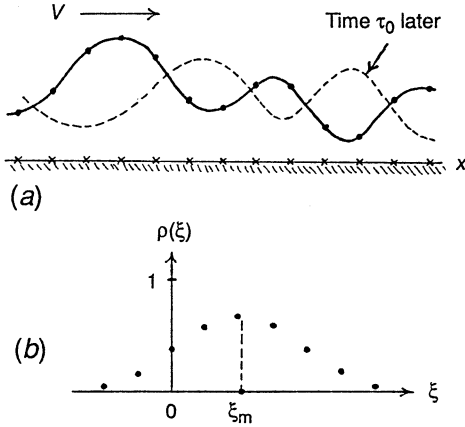


Fig. 3. (a) A moving and changing pattern is observed by a row of equally spaced antennas represented by crosses. (b) The form of the correlation function expected when cross-correlating the two patterns observed at times $t = 0$ and τ_0 . The maximum correlation occurs for a spatial shift ξ_m .

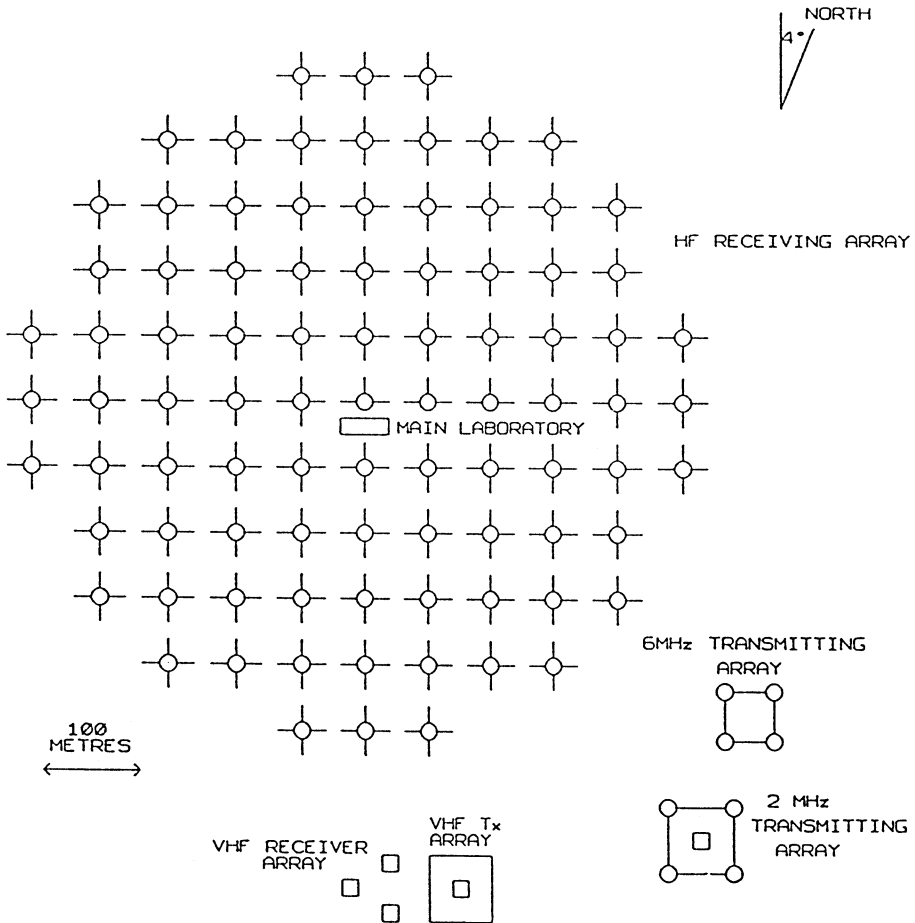


Fig. 4. Plan view of the Buckland Park antenna array. Note the transmitting antennas adjacent to the main receiving array.

the correction for random changes was quite important, and the true velocity was often considerably less than the apparent velocity. In view of the somewhat arbitrary assumptions of the model it was not universally accepted as a method for obtaining the true velocity.

3. Work at Adelaide: The Buckland Park Array

In 1962 I left Cambridge and joined the Department of Physics at the University of Adelaide. Dr W. G. Elford was already measuring winds in the height range 80–100 km using a meteor radar technique (Elford 1959). It seemed appropriate to supplement these observations using the spaced-antenna technique. However, the technique was controversial for the reasons mentioned above, and there were even concerns about the validity of the point-source effect. It appeared that both these issues could be settled one way or the other by building a large array of receiving antennas, so that the pattern motion could be observed more directly.

The idea is illustrated in Fig. 3. Again, I will use the one-dimensional case for illustration. Fig. 3*a* shows the pattern moving in the x -direction with velocity V and changing as it moves. The pattern is shown at two times, $t = 0$ and τ_0 . The crosses represent a line of receiving antennas, equally spaced along the ground. With such an array we can actually determine the form of the pattern at the two times, and then plot a cross-correlation function by displacing the two curves relative to each other and plotting the correlation as a function of spatial shift. The expected form of this function is shown in Fig. 3*b*. The maximum correlation occurs at some shift ξ_m , say, but it is less than unity because the pattern has changed its form in the time τ_0 . However, since this method of analysis introduces no time shifts, the value of ξ_m is not subject to bias by the random changes. The true velocity is therefore given by $V = \xi_m/\tau_0$.

In practice a two-dimensional array of antennas will be required, and the vectorial displacement of the pattern in the time τ_0 must be determined. If this displacement is \mathbf{r}_m , then the true vectorial velocity \mathbf{V} is given by

$$\mathbf{V} = \frac{\mathbf{r}_m}{\tau_0}. \quad (11)$$

By building a large array of antennas, it would be possible, then, to compare the velocity obtained from (11) with that obtained using only three antennas of the array, using the more controversial correlation analysis to correct for the effect of random changes.

Dr Elford and I together designed a suitable array, to operate at 2 and 6 MHz. Situated about 40 km north of Adelaide, it has become known as the Buckland Park array. We knew that the array would have to be at least $1 \times 1 \text{ km}^2$ in size in order to encompass several maxima of the diffraction pattern on the ground. We finally decided on a circular shape 1 km in diameter containing 89 pairs of crossed dipoles (Fig. 4). Each of the dipoles has its own buried coaxial feeder line running to the central laboratory. There the outputs of 89 radio receivers were digitised and recorded on magnetic tape. The output voltages were also used to control the brightness of 89 light globes, arranged in the same configuration as the antennas, so that the motion of the pattern over the ground was made visible. A piece of ground glass placed over the globe array acted as a diffuser

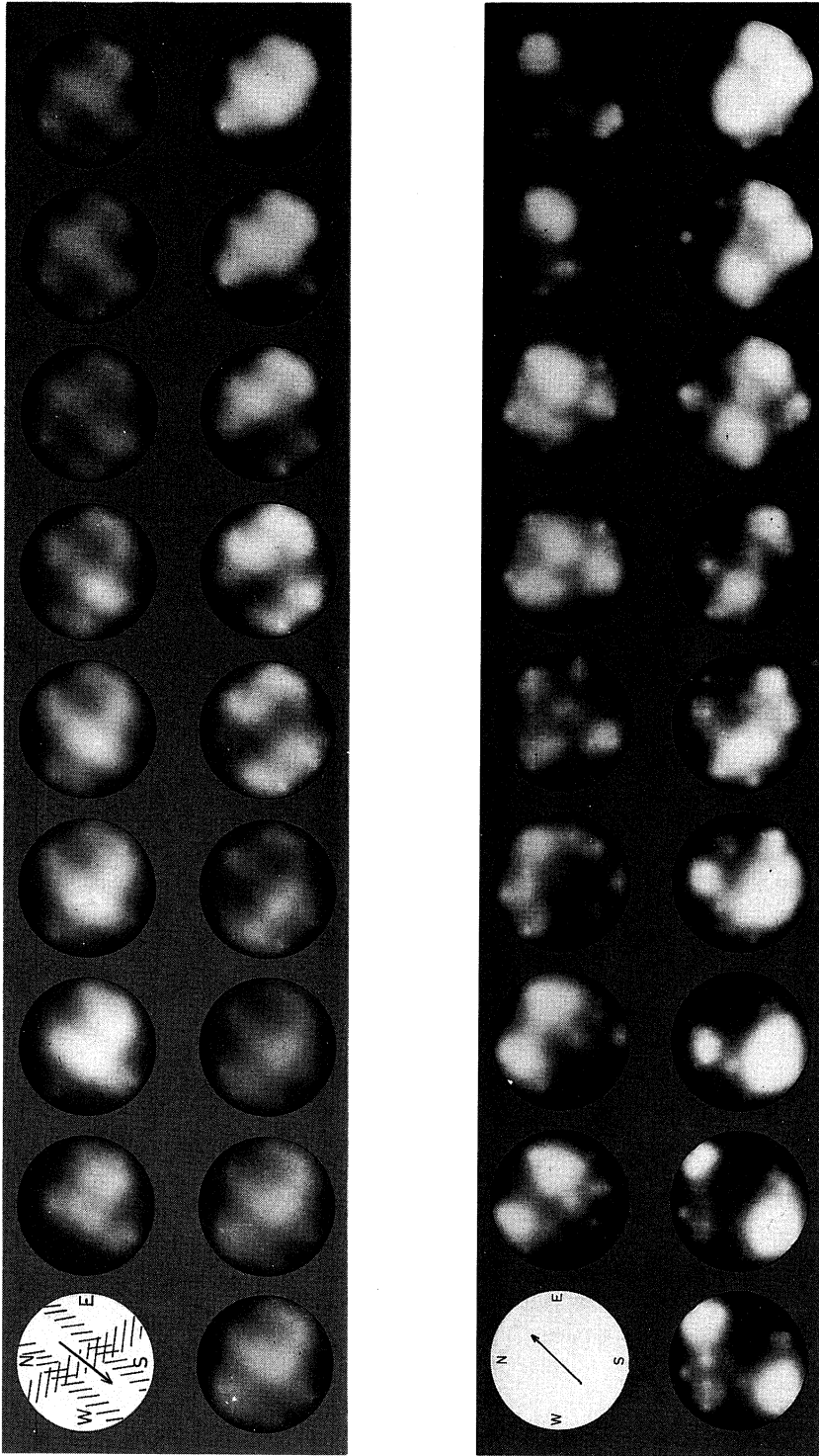


Fig. 5. *Top:* A sequence of patterns recorded at 0.75 s intervals when reflection was from a sporadic E layer at a height of 100 km. *Bottom:* A sequence of patterns recorded at 0.5 s intervals when the radio echo was from weak scattering irregularities at a height of 96 km. Direction of pattern motion is indicated in the top left-hand corner. (After Felgate 1970.)

and produced a smooth picture. The moving pattern could be photographed with a cine-camera. Transmitting arrays consisting of four dipoles each were situated adjacent to the large array (Fig. 4).

Construction commenced in 1965 and the first results were obtained in 1968 (Briggs *et al.* 1969). Golley and Rossiter (1970) showed that the velocity obtained using three antennas agreed well with the velocity obtained using the whole array, provided the effects of random changes were allowed for, and provided the spacing of the three antennas was not too small. This was an important result, because it meant that the more economical three-antenna method could be adopted as a routine technique. Felgate (1970) was able to verify the correctness of the point-source effect in the following way. A low-power transmitter was switched rapidly from one antenna of the large array to an adjacent one, a distance of 91 m. The rest of the array was used to observe the resultant motion of the whole diffraction pattern, which was found to be 91 m in the opposite direction. As explained earlier, this is geometrically equivalent to the point-source effect, and it justifies dividing the pattern velocities by a factor of 2, as Pawsey did, in order to obtain the wind in the upper atmosphere.

Fig. 5 shows two types of pattern revealed by the globe display. Fig. 5 (top) is a sequence of patterns, recorded at 0.75 s intervals, when reflection was from the ionospheric sporadic-E layer at a height of 100 km. Close inspection shows that the pattern is dominated by sets of parallel fringes, as sketched in the top left-hand corner. The sporadic-E layer was totally reflecting, and probably distorted by wave motions, so that multiple reflection points occurred. Each pair of reflection points will produce a set of Young's interference fringes. Since the pattern motion is dominated by the motion of these fringes, such occasions are not suitable for measuring the wind at the reflection level.

By contrast, Fig. 5 (bottom) shows patterns obtained when the echo was due to weak partial reflections from a height below the E region. These echoes, which occur in the height range 60 km upwards, were studied by Gardner and Pawsey (1953). The patterns are seen to be of a random form; in fact fringes were never observed when using these weak scatter echoes (Felgate and Golley 1971). The velocity obtained at these heights should be reliable, and should represent the wind in the neutral air, because the collision frequency between ions and neutrals is large enough to ensure that the ionised irregularities are carried along by the wind.

The extension of the spaced-antenna technique to utilise the weak partial reflections was an important advance, because it enabled winds to be observed simultaneously over a wide range of heights. The method was pioneered by Fraser (1965) at Christchurch, New Zealand. Because of the weakness of the echoes it requires the use of high transmitter powers and sensitive radio receivers.

Dr R. A. Vincent joined the University of Adelaide group in 1970. He has continued to develop and improve the spaced-antenna technique. An important advance was to make use of the phase as well as the amplitude of the echoes. Coherent detectors provide in-phase and quadrature components, and the signals are coherently integrated over a number of pulses to improve the signal-to-noise ratio. Winds are computed in real time every 2 minutes and at 2 km height intervals in the 60–95 km height range. The system can operate unattended.

This facility has produced an extremely valuable data base which can be analysed to give information about atmospheric dynamics on many different time scales. The prevailing winds are important for studies of the general circulation of the atmosphere. Planetary-scale waves, having periods in the range 2–5 days, can be studied. Tidal oscillations with both the solar and lunar periods are evident in the data, and can be used to test theoretical models. The shortest period variations in the winds, with periods as short as 5 min, are due to internal gravity waves. The importance of wave motions in coupling different levels of the atmosphere by transport of energy and momentum will be discussed later (Section 7). It is impossible to discuss all these results in the present paper and I must refer the reader to the following reviews: Vincent (1984*a*, 1984*b*, 1990).

In 1985 a small VHF radar operating on 54 MHz was constructed adjacent to the main Buckland Park array (see Fig. 4). It has a $90 \times 90 \text{ m}^2$ transmitting antenna and three spaced receiving antennas. It measures winds in the height range 2–15 km by the spaced-antenna technique, making use of scattering from inhomogeneities in the neutral atmosphere (Vincent *et al.* 1987). The introduction of the spaced-antenna radar technique for observations in this height range is due to Vincent and Röttger (1980).

4. Image Forming

Patterns such as those shown in Fig. 5 are of limited value for studying the nature of the atmospheric scatterers. They are Fresnel diffraction patterns, and the details can be expected to bear little relation to the actual structure in the atmosphere. A focussing or imaging system is needed, and such a system must make use of both the phase and the amplitude at each point in the pattern.

Fig. 6 shows how this was achieved, using processing by ultrasonic waves (Briggs and Holmes 1973; Holmes 1975). The intermediate frequency outputs of each of 89 receivers, at a frequency of 455 kHz, were used to drive a set of piezoelectric transducers, arranged in the same configuration as the 89 dipole antennas of the array. This array of transducers was at the top of a cylindrical water tank. At the bottom of the tank a similar array of transducers converted the acoustic signals back into voltages. Imagine, for the moment, that an ‘acoustic lens’ is placed in the tank one focal length above the bottom. Then the upper transducer array will launch a wave which is focussed by the lens onto the array at the bottom of the tank. For example, reflection from a perfectly smooth horizontal ionospheric layer would induce equal phases and amplitudes in each of the transmitting transducers at the top of the tank, and the wave launched into the tank would focus to a point at the centre of the lower transducer array. A plane wave arriving from some off-zenith angle would induce voltages having a linear phase gradient across the upper transducer array, and this would focus to a point displaced from the centre of the lower array. The geometrical factors were arranged in such a way that the edge of the lower array corresponded to a real off-zenith angle of 28° .

How is the ‘acoustic lens’ in Fig. 6 to be produced? Fortunately it was not needed; the diagram is only schematic. The effect of a lens was produced by arranging the upper transducers to be on the surface of a sphere, whose centre was at the centre of the lower array. The final image was made visible with an array of light-emitting diodes, and the voltage for each image point was also digitised and recorded on magnetic tape.

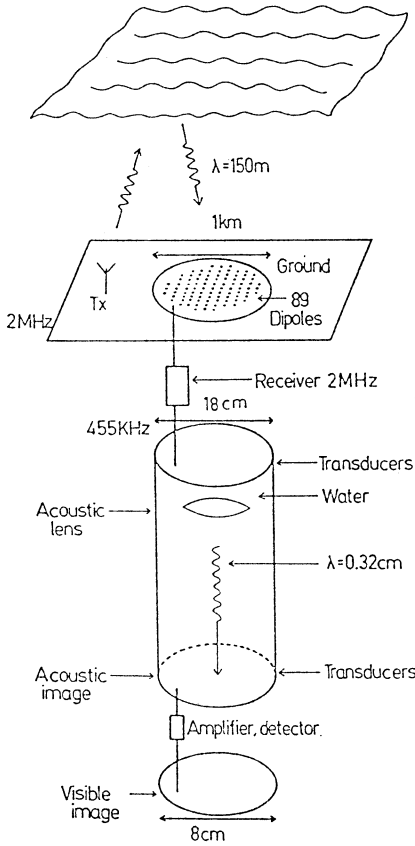


Fig. 6. Schematic diagram of the ultrasonic image-forming system (see text for a full description).

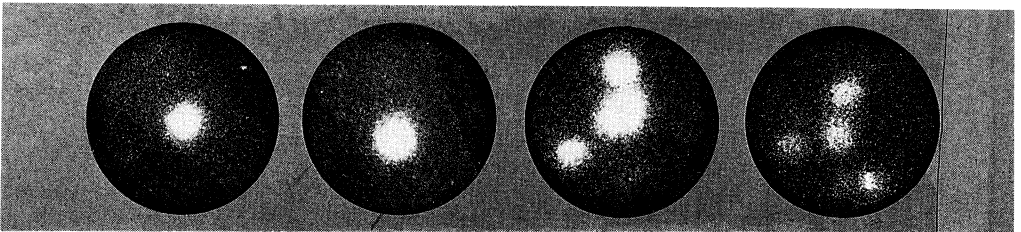


Fig. 7. Images produced by the ultrasonic image former when the echoes were from totally reflecting ionospheric layers. *Left to right:* a single reflection point at the zenith; a single reflection point off-zenith (indicating layer tilt); three reflection points (indicating a distorted reflecting surface allowing multiple 'glints'); and four reflection points.

Fig. 7 shows some images produced by the image former. Reflections were from totally reflecting ionospheric layers and, as anticipated, the images show multiple reflection points or 'glints', but with the main reflection coming from close to the zenith. Unfortunately, the system could not be made sensitive enough to study the weak partial reflections in the height range 60–95 km which are used to measure winds. Also, the system was difficult to maintain.

The ultrasonic image former is an analogue computer for two-dimensional Fourier transforms. It is a parallel computer; all image points are computed simultaneously. The transducers and water tank could now be replaced with a digital computer. However, it would still be a somewhat formidable task to maintain 89 sensitive radio receivers, which must have stable gains and phase shifts. It is a project which the group would like to pursue again at some future time, and there are tentative plans to use 30 receivers, each connected to three dipoles of the array (see Section 8).

5. Measurement of Atmospheric Turbulence

In the early 1980s, Dr W. K. Hocking began measuring atmospheric turbulence at Adelaide using a radar technique. The basic idea was simple. If radar echoes are returned from atmospheric scatterers with varying velocities, the spectrum of the returned signals will be broadened by the Doppler effect. Measurement of the spectral width will give information about the magnitude of the random velocities and hence about the intensity of the turbulence.

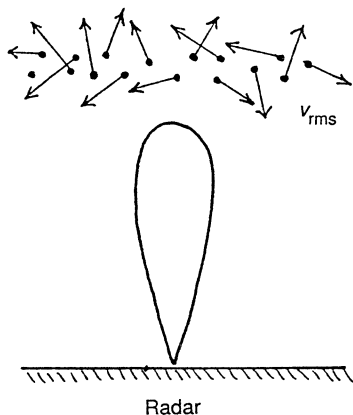


Fig. 8. Schematic diagram representing radar scattering from a set of scatterers with random turbulent velocities. (The real scatterers will not be point-like.)

Fig. 8 shows schematically a set of scatterers which have random turbulent motions with r.m.s. velocity v_{rms} . The actual probability distribution of v_r , the velocity component in a specified radial direction (in this case vertical), is assumed to be given by

$$p(v_r) \propto \exp\left(-\frac{v_r^2}{2v_{rms}^2}\right). \quad (12)$$

A scatterer with outward radial velocity v_r will produce a Doppler shift given by

$$f = -\frac{2}{\lambda} v_r, \quad (13)$$

where λ is the radar wavelength and f is the change in frequency relative to the transmitted frequency.

The power spectrum $W_t(f)$ due to turbulence alone is obtained by substituting v_r from (13) into (12), giving

$$W_t(f) \propto \exp\left(-\frac{\lambda^2 f^2}{8v_{\text{rms}}^2}\right) = \exp\left(-\frac{f^2}{f_t^2}\right), \quad (14)$$

where f_t is the e^{-1} half-width of the power spectrum. Thus by measuring f_t , v_{rms} can be found from

$$v_{\text{rms}} = \lambda f_t / 2\sqrt{2}. \quad (15)$$

This procedure is the same as that used to find the temperature of a gas by measuring the thermal broadening of an emission line.

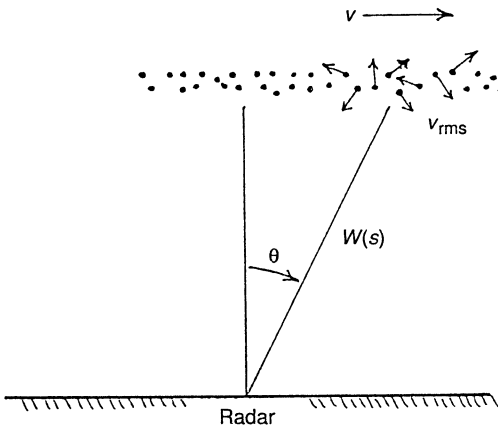


Fig. 9. Schematic diagram representing the situation when the scatterers have random turbulent velocities and are also transported by a constant horizontal wind. Here $W(s)ds$ is the power returned from the range s to $s + ds$, where $s = \sin \theta$.

If this were the full story, the technique would be simple. Unfortunately, a serious complication arises because of the presence of the horizontal wind. Fig. 9 shows schematically the situation when the atmospheric scatterers have a mean velocity v and an r.m.s. turbulent velocity v_{rms} . Here $W(s)$ represents the power returned as a function of angle, where $s = \sin \theta$. For narrow antenna polar diagrams, this will depend mainly on the radar polar diagram, rather than on the scatterers themselves, and can therefore be assumed to be known. In fact, Hocking showed that a good approximation to the power polar diagram of the whole Buckland Park antenna array, with all elements connected in phase, is the Gaussian of equation (9), where s_0 is a measure of the half-width of the beam, and he used the array in this way as a receiving antenna. Now, a radio wave arriving at a zenith angle θ will have a Doppler shift due to the horizontal wind v given by

$$f = -\frac{2}{\lambda}v \sin \theta = -\frac{2vs}{\lambda}. \quad (16)$$

(Of course, the real two-dimensional case is more complicated; see Hocking 1983*a*.) The power spectrum $W_v(f)$ due to the wind alone is found by substituting s

from (16) into (9), giving

$$W_v(f) \propto \exp \left\{ - \left(\frac{f\lambda}{2vs_0} \right)^2 \right\} \\ \propto \exp \left(- \frac{f^2}{f_v^2} \right), \quad (17)$$

where

$$f_v = 2vs_0/\lambda. \quad (18)$$

The quantity f_v is the e^{-1} half-width of the power spectrum due to the effect of the wind alone. Since s_0 for the large antenna array is known, and v can be measured with a spaced-antenna experiment, we can assume that f_v is known.

Now the observed power spectrum of the returned signal will be a convolution of the effects of wind and turbulence. This can be seen by considering the signal arriving at a zenith angle θ . This has a mean Doppler shift given by (16) together with a 'spread' given by (14). For each direction the signals are spread in frequency due to the turbulence, and these spread contributions must be added to give the resultant power spectrum. This is the classical definition of a convolution (e.g. Bracewell 1965). Thus we can write for the resultant power spectrum $W_{tv}(f)$ due to both turbulence and wind

$$W_{tv}(f) \propto \exp \left(- \frac{f^2}{f_v^2} \right) \otimes \exp \left(- \frac{f^2}{f_t^2} \right), \quad (19)$$

where \otimes represents a convolution. It can easily be shown that $W_{tv}(f)$ is also Gaussian with an e^{-1} half-width f_0 given by

$$f_0^2 = f_v^2 + f_t^2. \quad (20)$$

Thus, since f_0 can be measured and f_v is known, f_t can be found. The r.m.s. turbulent velocity then follows from (15).

In practice, the correction for f_v is often large, so that the required f_t^2 is the small difference between two large quantities. To make f_v as small as possible, we need a narrow polar diagram for the receiving antenna (s_0 small). This was why the Buckland Park array was so useful for this work; it is the largest array of its type in the world for work at medium frequencies. This use was certainly not envisaged when it was designed.

Typical results obtained for v_{rms} in the height range 60–95 km are of the order of 3 m s^{-1} . This corresponds to a turbulent energy dissipation rate of about 0.1 W kg^{-1} . Of course the results vary with height and time, and Hocking has made a detailed study of turbulence in this height range (Hocking 1983*a*, 1983*b*, 1985, 1988, 1990). The above is an over-simplified account of his work, for which he was awarded the Pawsey Medal of the Australian Academy of Science in 1990.

6. Analysis in the Frequency Domain

It is interesting to note that the approach described in Section 5 contains the same physical content as the ‘correlation analysis’ of Section 2. That is, both include the effects of a uniform horizontal wind, together with turbulent motions of the individual scatterers. The only difference is that in Section 2 the description was in the time domain, through the use of auto- and cross-correlation functions of the time series, while in Section 5 the description was in the frequency domain, through the use of the power spectrum. It is therefore of interest to see whether the two approaches are actually equivalent.

The Wiener–Khinchine theorem tells us that the autocorrelation function is the Fourier transform of the power spectrum. This suggests taking the Fourier transform of (19). The left-hand side gives us the autocorrelation function, and the right-hand side, by the convolution theorem, becomes the *product* of the Fourier transform of the two Gaussians. Thus, we have

$$\rho_{11}(\tau) \propto \exp(-\pi^2 f_v^2 \tau^2) \exp(-\pi^2 f_t^2 \tau^2). \quad (21)$$

This is, indeed, of the same form as (8) with the constants related as follows:

$$\pi^2 f_v^2 = \frac{V^2}{\xi_1^2}, \quad (22)$$

$$\pi^2 f_t^2 = \frac{1}{\tau_1^2}. \quad (22)$$

Equation (22) follows immediately from (10) and (18), remembering that $V = 2v$. Equation (23) is the expected relation between the width of the power spectrum (for an observer moving with the pattern) and the pattern lifetime, in view of the fact that the power spectrum is the Fourier transform of the autocorrelation function.

Thus, it appears that the two approaches are equivalent. The physical basis of the theory is much clearer, however, when it is formulated in the frequency domain than in the time domain. Perhaps if it had been formulated in this way in the 1950s it would have been less controversial.

This naturally raises the question as to whether the whole analysis can be carried out in the frequency domain. If the turbulent intensity can be obtained from the corrected power spectrum, then can the horizontal wind be found from the cross spectrum, which is the Fourier transform of the cross-correlation function? The answer is that it can, and there has recently been considerable interest in this possibility. Some formulations give only the apparent velocity, but Briggs and Vincent (1992) have recently shown how the true velocity can be obtained from an analysis which is the exact frequency-domain equivalent of the standard time-domain analysis. Since the two methods are mathematically equivalent, the frequency domain method cannot give anything new, but it may have practical or computational advantages. One such advantage is that when using it, interference occurring on specific known frequencies can easily be removed.

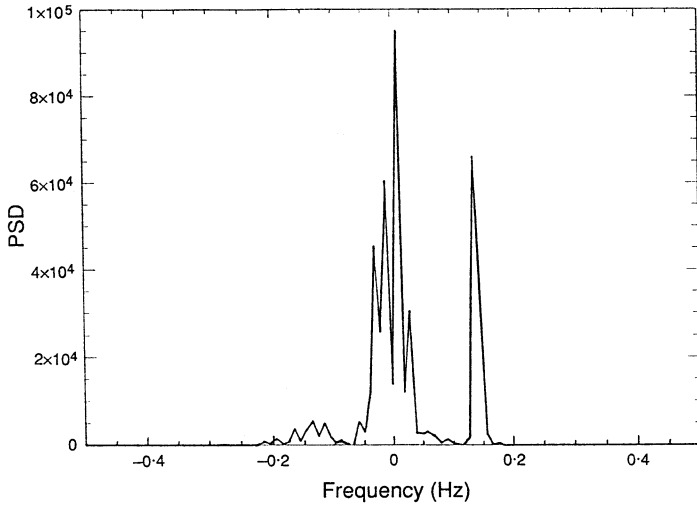


Fig. 10. Power spectral density (PSD) of echoes returned from a range of 86 km at Christmas Island. The strong peak at 0.14 Hz is produced by echoes from the surface of the sea. ('Frequency' indicates frequency offset from the transmitted frequency.)

An example of such interference is that arising from sea echoes. The Adelaide group operates a radar at Christmas Island ($2^{\circ}\text{N}, 157^{\circ}\text{W}$) (Vincent and Lesicar 1991). As it is completely surrounded by sea, it is particularly susceptible to interference by echoes reflected from the surface of the sea, due to a small leakage of radiation in the horizontal direction. Sea echoes occur when the sea surface has a significant Fourier component aligned perpendicular to the line of sight and with a wavelength equal to one-half the radar wavelength, since such a component satisfies the Bragg reflection condition. Now in deep water, sea waves of a specified wavelength always travel at the same known speed and therefore produce a known Doppler shift. For the 2 MHz radar at Christmas Island the expected Doppler shift is 0.14 Hz. Fig. 10 shows a power spectrum of the echoes returned from a range of 86 km. The spread of power around 0 Hz is due to the atmospheric scatterers at a height of 86 km, but a narrow peak at 0.14 Hz can also be seen. This is the power scattered back from the sea surface at a horizontal distance of 86 km from the radar. For the example of Fig. 10 this sea scatter would not be much of a problem, because it is well separated in frequency from the wanted signal. However, the atmospheric signal is sometimes spread over a much wider frequency band, and the sea scatter may be in the middle of it. It is easily eliminated by giving frequencies close to 0.14 Hz zero weight in any statistical procedures which are applied to the data. Such filtering can be done in the time domain also, but it is much easier to do it when working in the frequency domain.

7. Measurements of Vertical Flux of Horizontal Momentum

During the last decade or so it has been realised that conventional driving forces are unable to explain the general circulation of the atmosphere, and that a probable explanation of the discrepancy is momentum transport by waves. A familiar example of how waves can deposit momentum is the breaking of waves

on a beach. The fact that objects can be transported up the beach shows that considerable momentum is being released. In the atmosphere internal gravity waves are generated near the Earth's surface by various processes such as storms, cold fronts and winds blowing over mountains. The waves then travel upwards and actually grow in amplitude in order to preserve energy as the density of the atmosphere decreases. (The kinetic energy per unit volume is $\frac{1}{2}\rho u'^2$, where ρ is the density and u' the perturbation air velocity due to the wave. Thus as ρ decreases u' must increase.) Eventually the waves are either absorbed or reach such large amplitudes that they 'break'. In either case, the momentum and energy are deposited, leading to acceleration and heating of the atmosphere. The effects in the 60–95 km height range are large due to the fact that the waves are generated near the ground where the density is high, and they deposit their energy and momentum in a region where the density is smaller by a factor of the order of 10^5 or 10^6 .

The horizontal momentum per unit volume due to the wave is $\rho u'$, and if the upward perturbation air velocity is w' , the mean vertical flux of horizontal momentum is $\overline{\rho u' w'}$, where the overbar denotes a time average. Of course, a constant flux of momentum passing through a region will not produce any acceleration; it is the divergence of the flux which causes a net deposition of momentum and hence an acceleration. It can be shown that the force per unit mass F (i.e. the horizontal acceleration) is given by

$$F = -\frac{1}{\rho} \frac{d}{dz} (\overline{\rho u' w'}). \quad (24)$$

Note that ρ is a function of height z , and so it does not cancel out; the variation of ρ with z can be obtained from a model atmosphere.

It seems unlikely that it will ever be possible to develop a theory to predict the vertical flux of momentum on a global scale, because of the capricious nature of the wave sources, and the fact that small scale waves cannot be included in global numerical models. A method for measuring the flux directly is required, and for this measurements of $\overline{u' w'}$ as a function of height are needed. In the early 1980s Vincent and Reid (1983) devised a method for using the Buckland Park array to do this. It is another use for the array which was certainly not thought of when the array was first designed.

The principle of the method is shown in Fig. 11. Two beams are generated at angles $\pm\theta$ on either side of the zenith, using all 89 elements of the array with suitable phasing. The radial velocity fluctuations produced by gravity waves are measured for these two directions by determining the mean Doppler shifts of the radar echoes as a function of time. Let these velocities be $v(\theta, R)$ and $v(-\theta, R)$, where R is the range selected by the radar. Then, by writing down the expressions for the radial components of the perturbation air velocities u', w' , it can be shown that (Vincent and Reid 1983)

$$\overline{u' w'} = \frac{\overline{v^2(\theta, R)} - \overline{v^2(-\theta, R)}}{2 \sin 2\theta}, \quad (25)$$

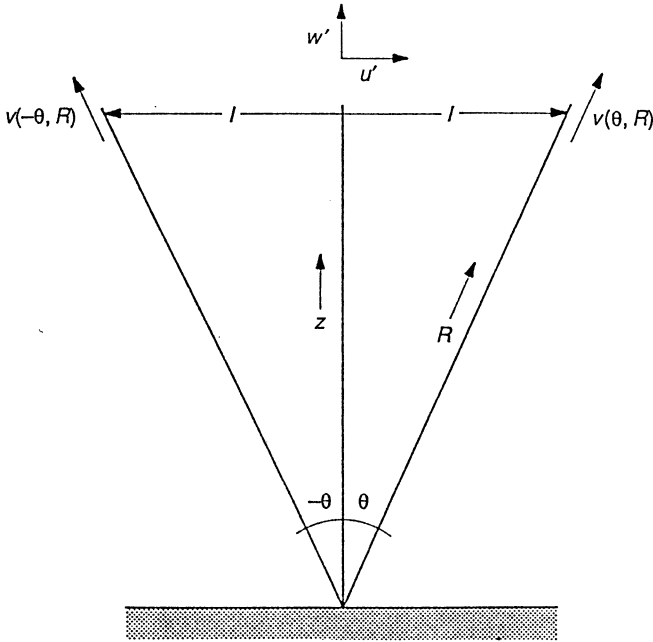


Fig. 11. Twin-beam technique for measuring the vertical flux of horizontal momentum.

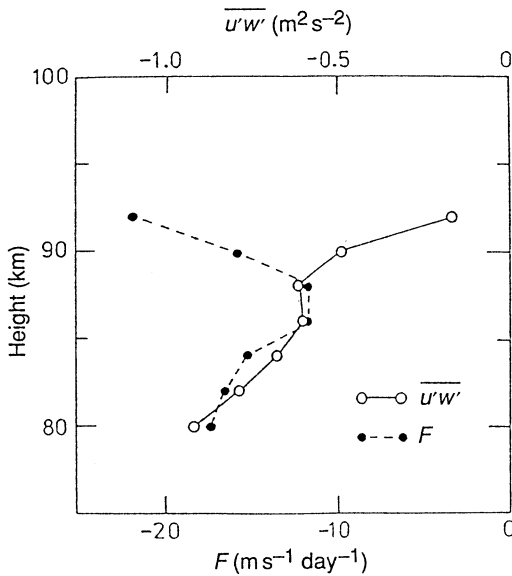


Fig. 12. Open circles show the vertical variation of the measured values of $\overline{u'w'}$ (upper scale). The solid circles show the derived values of acceleration F (lower scale). (After Vincent and Reid 1983.)

where the overbars represent time averages. Since $z = R \cos \theta$, and different ranges can be selected by the radar, (25) enables $\overline{u'w'}$ to be determined as a function of height z . This can then be used in (24) to find F .

Typical results are shown in Fig. 12. The measured flux $\overline{u'w'}$ and the derived values of F are both shown as functions of height over the range 80 to 92 km. The flux and the acceleration are both negative, indicating a westward acceleration. The magnitude is of the order of 15 ms^{-1} per day. This is very significant, and quite comparable with the accelerations produced by other forces which drive the general circulation. More recent results can be found in Fritts and Vincent (1987) and Reid and Vincent (1987).

It is very important to understand the general circulation of the atmosphere in order to be able to model possible changes due to anthropogenic effects such as increasing carbon dioxide. General circulation models certainly cannot neglect momentum transport by waves, but such effects will have to be included by empirical parametrisations, based on measurements. Radar techniques are therefore very important.

8. Future Plans

The Buckland Park array has some limitations. In spite of its large size the beamwidth using all 89 elements at 2 MHz is $\pm 4.5^\circ$ to half power. A narrower beam than this would lead to improvements in turbulence measurements and also in momentum flux measurements, because the off-zenith angles would be more accurately defined. The same is true for measurements of horizontal winds by a Doppler technique using off-zenith beams (not discussed in this paper). Also, at present the beam-forming techniques are based on the use of 'plug-in' cables which have to be set up manually—a time-consuming process.

When it was designed in the 1960s, the array was a large project which stretched available finances to the utmost. For economy reasons, it was designed to be used only for reception. The radar transmitting antennas were small and quite separate from the large array (see Fig. 4). If the whole array could be used also for transmission (and most radars do use the same antenna for transmission and reception), the effective beamwidth would be decreased, and the sensitivity would be increased.

A complete redesign along these lines is at present being implemented, under the direction of Dr I. M. Reid. It is planned to use 30 modular transmitters, each driving a section of the array. The power-aperture product will be increased by two orders of magnitude over the present value. Computer-controlled beam forming will be incorporated in place of the present cable systems, so that rapid beam changing will be possible. Previous observations will be continued with greater precision and sensitivity, and new types of observations will become possible. A digital image-forming technique may be used, with 30 radio receivers, each connected to three dipoles of the array.

9. Discussion

Any tracing of the history of a technique by following developments in one research group is bound to be unbalanced. In this review I have not, in general, mentioned the important contributions made by workers in other groups. I would therefore like to end by stressing that cooperation between groups is especially important in atmospheric physics, because of the global nature of the phenomena. Coordinated campaigns of simultaneous observations are invaluable. The University of Adelaide group does have close links with other groups, both

in Australia and overseas. In some cases, portable experiments are brought and set up adjacent to the Buckland Park array. We are most grateful for this collaboration which exists with other university groups in Australia, and with CSIRO, the Bureau of Meteorology, and DSTO. We also have valuable cooperation with overseas groups in Japan, the USA, Germany, New Zealand and elsewhere. This type of cooperation has been well fostered by the present leader of the group, Dr R. A. Vincent, who is a member of many national and international committees, and is currently President of the International Commission for the Meteorology of the Upper Atmosphere.

Acknowledgments

I would like to thank all my present and former colleagues and students for their help over the years. I hope they will all feel that they have a share in the honour of the Harrie Massey Prize. The work of the Atmospheric Physics Group at the University of Adelaide is supported by the Australian Research Council.

References

- Bracewell, R. N. (1965). 'The Fourier Transform and Its Applications' (McGraw-Hill: New York).
- Briggs, B. H. (1984). In 'Handbook for the Middle Atmosphere Program', Vol. 13, p. 166 (SCOSTEP Secretariat: Univ. Illinois, Urbana).
- Briggs, B. H., Elford, W. G., Felgate, D. G., Golley, M. G., Rossiter, D. E., and Smith, J. W. (1969). *Nature* **223**, 1321.
- Briggs, B. H., and Holmes, N. (1973). *Nature Phys. Sci.* **243**, 111.
- Briggs, B. H., Phillips, G. J., and Shinn, D. H. (1950). *Proc. Phys. Soc. London B* **63**, 106.
- Briggs, B. H., and Vincent, R. A. (1992). *Radio Sci.* **27**, 117.
- Elford, W. G. (1959). *J. Atmos. Terr. Phys.* **15**, 132.
- Felgate, D. G. (1970). *J. Atmos. Terr. Phys.* **32**, 241.
- Felgate, D. G., and Golley, M. G. (1971). *J. Atmos. Terr. Phys.* **33**, 1353.
- Fraser, G. J. (1965). *J. Atmos. Sci.* **22**, 217.
- Fritts, D. C., and Vincent, R. A. (1987). *J. Atmos. Sci.* **44**, 605.
- Gardner, F. F., and Pawsey, J. L. (1953). *J. Atmos. Terr. Phys.* **3**, 321.
- Golley, M. G., and Rossiter, D. E. (1970). *J. Atmos. Terr. Phys.* **32**, 1215.
- Hocking, W. K. (1983a). *J. Atmos. Terr. Phys.* **45**, 89.
- Hocking, W. K. (1983b). *J. Atmos. Terr. Phys.* **45**, 103.
- Hocking, W. K. (1985). *Radio Sci.* **20**, 1403.
- Hocking, W. K. (1988). *J. Geophys. Res.* **93**, 2475.
- Hocking, W. K. (1990). *Adv. Space Res.* **10**, 153.
- Holmes, N. (1975). *Proc. IREE (Aust.)* **36**, 321.
- Pawsey, J. L. (1935). *Proc. Camb. Phil. Soc.* **31**, 125.
- Phillips, G. J., and Spencer, M. (1955). *Proc. Phys. Soc. London B* **68**, 481.
- Ratcliffe, J. A. (1956). *Rep. Prog. Phys.* **19**, 188.
- Reid, I. M., and Vincent, R. A. (1987). *J. Atmos. Terr. Phys.* **49**, 443.
- Vincent, R. A. (1984a). *J. Atmos. Terr. Phys.* **46**, 119.
- Vincent, R. A. (1984b). *J. Atmos. Terr. Phys.* **46**, 961.
- Vincent, R. A. (1990). *Adv. Space Res.* **10**, 93.
- Vincent, R. A., May, P. T., Hocking, W. K., Elford, W. G., Candy, B., and Briggs, B. H. (1987). *J. Atmos. Terr. Phys.* **49**, 353.
- Vincent, R. A., and Lesicar, D. (1991). *Geophys. Res. Lett.* **18**, 825.
- Vincent, R. A., and Reid, I. M. (1983). *J. Atmos. Sci.* **40**, 1321.
- Vincent, R. A., and Röttger, J. (1980). *Radio Sci.* **15**, 319.

